Towards sustainable textile waste management: Exploring valuable chemicals production through steam cracking in a dual fluidized bed

Fuel 397 (2025) 135731

Contents lists available at ScienceDirect

Fuel

journal homepage: www.elsevier.com/locate/fuel

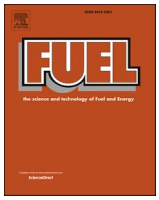

Full Length Article

Towards sustainable textile waste management: Exploring valuable chemicals production through steam cracking in a dual fluidized bed☆

Renesteban Forero-Franco [a,*], Isabel Cañete-Vela [b], Teresa Berdugo-Vilches [a], Chahat Mandviwala [a], Nidia Díaz Perez [a], Ivan Gogolev [a], Henrik Thunman [a], Martin Seemann [a]

[a] Department of Space, Earth and Environment (SEE), Division of Energy Technology, Chalmers University of Technology, 41296 Gothenburg, Sweden
[b] Borealis AB, 444 86 Stenungsund, Sweden

ARTICLE INFO

Keywords:
Textile waste recycling
Steam cracking
Dual fluidized bed
Large-scale experiments
Valuable chemicals
Closed-loop recycling
Household textile waste

ABSTRACT

Global demand for textiles is rising due to population and economic growth, yet most end-of-life textiles are incinerated or landfilled, posing environmental risks. In Europe, less than 1 % of discarded textiles are recycled into materials of similar quality. Thermochemical recycling, such as steam cracking, offers a potential solution by breaking down polymer chains at high temperatures to produce valuable chemicals and reduce dependence on fossil fuels. This study explores the potential of producing valuable chemicals from steam cracking of textile waste in a semi-industrial dual fluidized bed (DFB) reactor powered by biomass. Experiments were conducted at temperatures ranging from 735° to 815 °C using polyester- and cotton-based materials rejected from textile sorting processes. Results showed effective conversion of heterogeneous feedstocks into syngas, light monomers (ethylene and propylene), and aromatic compounds like BTXS (benzene, toluene, xylenes, styrene) without need of extensive pre-sorting. Polyester-based textiles yielded an average carbon conversion of ~11 % for syngas, ~7% for light monomers, and ~17 % for BTXS. From a carbon conversion analysis, the yields varied with temperature and feedstock composition: higher temperatures favored carbon oxides, while BTXS and light monomers remained stable. PET-rich batches produced more CO_2 and aromatics, whereas cellulose-based feedstocks favored syngas production. Overall, steam cracking can achieve a carbon recovery rate of nearly 70 %, through valuable chemicals, syngas, and CO_2 utilization, significantly outperforming the ~3 % closed-loop recycling rate in current European schemes. These findings highlight the potential of steam cracking in DFB reactors as an alternative recycling method to enhance circularity in the textile industry.

1. Introduction

Textile production is one of the oldest and most significant sectors in the global economy. This industry encompasses a wide array of activities, from the production of raw fiber materials to the manufacturing of products such as clothes, shoes, and furniture, among others. However, the rapid growth of the textile industry as well as the mass production of inexpensive and cheap clothes crafted for short-term use, has raised concerns about the environmental impacts of its linear value chains, causing resource depletion and environmental pollution at all levels. The global production of textile fibers has increased from 58 million tonnes (Mt) in Year 2000 to 109 Mt in Year 2021. By Year 2030, it is projected to reach 149 Mt, reflecting the sector's rapid and continuous expansion [1]. This situation is evidently unsustainable and environmentally damaging.

In Europe (EU-27), approximately 15 kg of textile waste are generated per person annually, generating around 7 Mt of total textile waste each year. Most of the waste consists of clothes and home textiles,

Abbreviations: B1-3, Batch 1 to Batch 3; BTXS, Benzene, Toluene, Xylenes, styrene; $C-Al$, Carbons attached to Aliphatics; $C-AR$, Carbons attached to Aromatics; $C-_xO$, Carbons attached to Oxygen; $C-X$, Carbons attached to Heteroatoms; CCU, Carbon capture and utilization; Cell, Cellulose; DFB, Dual Fluidized Bed; FID, Flame Ionization Detector; GC, Gas Chromatographer; HTR, High Temperature Reactor; NDIR, Non-Dispersive Infrared Spectroscopy; NIR, Near Infrared Spectroscopy; PA, Polyamide; PAN, Polyacrylonitrile; PET, Polyethylene terephthalate; PP, Polypropylene; PVC, Polyvinyl chloride; SPA, Solid phase absorption; TGA, Thermogravimetric Analysis.

☆ This article is part of a special issue entitled: 'INFUB14' published in Fuel.

* Corresponding author.
E-mail address: rforero@chalmers.se (R. Forero-Franco).

https://doi.org/10.1016/j.fuel.2025.135731
Received 1 December 2024; Received in revised form 30 March 2025; Accepted 16 May 2025
Available online 24 May 2025

accounting for 85 % of the total. Regarding waste management, approximately 30 %–35 % by weight (%wt) of the total textile waste is collected for recycling [2]. Within this fraction, ~20 %–24 %wt is of sufficient quality to be reused, but a large fraction of it (~70–90 %wt, estimations for global north [3]) is exported to less-developed countries, eventually ending up in controlled or uncontrolled landfill sites [4]. Overall, ~9%–10 % of the waste textiles is directed to open-loop recycling processes, such as industrial rags or fuels, while only ~1 %wt participates in a closed-loop scheme involving fiber-to-fiber recycling (see Fig. 1). The remaining waste is either sent to landfills or incinerated for energy recovery [2].

In addition to the growing waste problem, the fashion industry is a relevant contributor to global greenhouse gas emissions, significantly impacting climate change. In 2018 alone, the industry released 2.1 gigatonnes of CO_2 equivalent into the atmosphere, accounting for approximately 4 % of global emissions. To put this in perspective, this is equal to the combined emissions of France, Germany, and the United Kingdom [6]. If current trends continue, the fashion sector could consume more than a quarter of the global carbon budget by 2050, threatening efforts to limit global warming to 2 °C [5]. Given this immense environmental footprint, there is a pressing need for innovative solutions and research aimed at reducing emissions within the fashion industry, particularly through the adoption of sustainable production methods and circular economy models.

Today's textiles are composed of synthetic and natural fibers, with a predominance of synthetic fibers. Synthetic fibers are primarily derived from fossil fuels, which presents a significant environmental challenge that must be addressed to reduce the industry's carbon footprint. Globally, 64 % of fiber production consists of synthetic fibers, such as polyester, polyamide, and polypropylene; 28 % comes from plant fibers as cotton, 6.4 % is man-made cellulosic fibers in the form of viscose, and 1.8 % comes from animal fibers as wool. Polyester dominates the market with a 54 % share of worldwide fiber production. Synthetic fibers are primarily fossil-based, with 87 % being sourced directly from oil and 13 % from recycled plastics [1]. In a business-as-usual scenario, the demand for fossil-based fibers is expected to increase by approximately 5.7 % annually. Therefore, to meet the climate goals set by the Paris Agreement [7], it is crucial to move away from the linear and wasteful value chain model by prioritizing circular solutions that reduce dependency on virgin fossil fuels and minimize the carbon footprint of textile production.

The complexity of textile waste streams, driven by fast fashion and the diverse composition of fibers, presents significant challenges for recycling. Current methods, such as mechanical recycling and solvolysis, work well for specific polymers but struggle with mixed or contaminated waste. Mechanical recycling relies on high fiber purity and uses shredding and carding to produce high-quality recycled fibers for closed-loop applications [2,5]. Since textiles often contain blends of synthetic and natural fibers, dyes, and additives, their processing becomes complicated and results in a large reject fraction of waste being diverted to open-loop recycling or incineration (see Fig. 1). In the case of polyester and nylon, solvolysis can efficiently and selectively depolymerize the fibers into valuable monomers [8], and even separate some polyester-cotton blends, offering a robust closed-loop solution [9]. However, it requires precisely matched solvents and reaction conditions, while contaminants like dyes and additives can reduce monomer quality and yield [10]. This inevitable leads to certain presorting requirements in the waste that usually leave a still significant reject fraction. These challenges in addressing the full spectrum of textile waste highlight the need for versatile recycling technologies capable of processing the kind of blended and heterogeneous textile mixtures found in waste or reject streams.

Thermochemical processes such as pyrolysis, gasification, and combustion coupled with carbon capture and utilization (CCU) have also been explored as potential recycling methods for textile waste. Pyrolysis is a general recycling method that breaks down polymers into pyrolysis oil, which can be used for energy production or as diesel-like fuels. However, the composition of the raw oil often limits its applicability to meet customer needs [11,12]. Catalytic pyrolysis with polymer-specific catalysts can recover valuable chemicals from certain polyester blends, but their effectiveness can be reduced for highly mixed waste streams [11,13], which makes it a selective process. Gasification, by contrast, converts textile waste into syngas (a mixture of CO and H_2) and is considered a general and robust technology for processing mixed textile waste among other recycling technologies [2,14], similar to combustion coupled with CCU for CO_2 recovery. Since the feedstock loses its molecular integrity, additional chemical synthesis steps are required to obtain back hydrocarbons from the syngas or CO_2, which significantly increases the overall techno-economic cost.

Given these limitations, alternative recycling technologies are

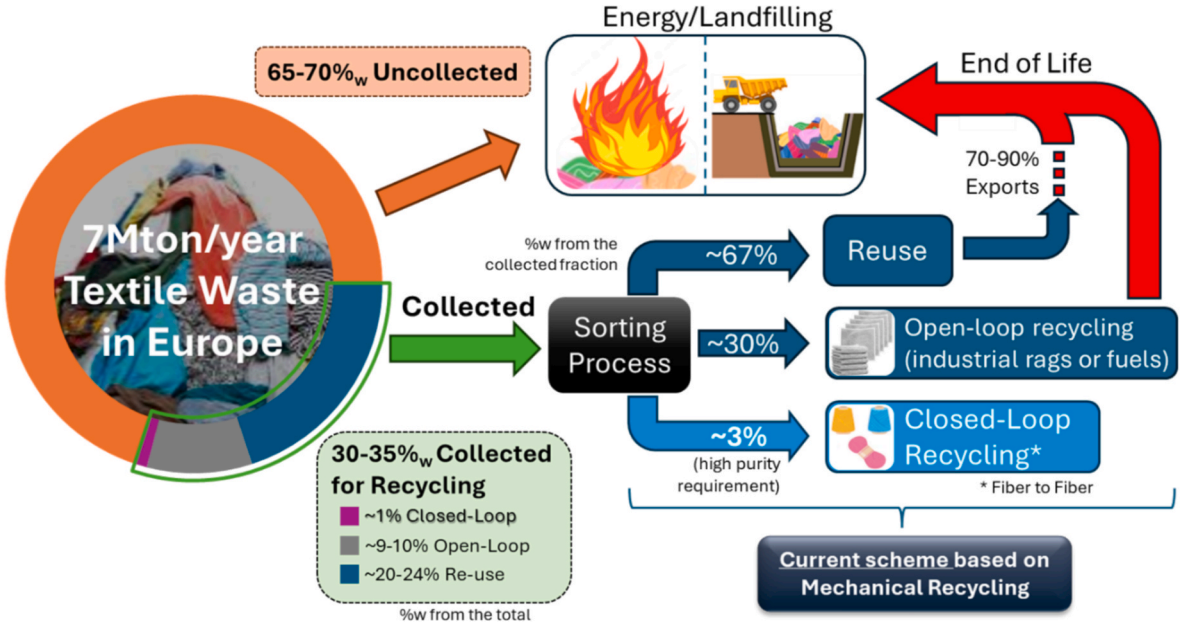

Fig. 1. Schematic of Europés textile waste management (data from (2022) [2,3,5]).

needed to manage the complex makeup of textile waste streams while maximizing the recovery of valuable components. Steam cracking, a well-established thermochemical process in the petrochemical industry, offers a promising solution. By breaking down polymer chains at high temperatures, it produces basic chemical components that can be separated downstream to create new materials. Steam cracking is highly versatile, capable of processing all kinds of heterogeneous feedstocks, including textiles with blended fibers and additives. This approach supports a closed-loop recycling model by ensuring that the carbon atoms from the waste remain within the production cycle to create new fibers and synthetic products, reducing the reliance on virgin raw materials.

The breakdown of carbon chains in the steam cracking process is endothermic. To optimize conversion and minimize unwanted by-products, key factors include steep thermal gradients, in situ dilution of products to reduce partial pressures, and short residence times within the reaction zone. One reactor concept that meets these requirements is the Dual Fluidized Bed (DFB) system, using steam as the fluidizing agent. DFB systems consist of a cracking reactor heated allothermally by a combustor, with a circulating heated sand bed acting as the heat carrier between the two units. They are distinguished by their high heat transfer rates to the feedstock and continuous ash removal via the sand circulation providing a robust reaction environment for thermochemical conversion. The dual-unit configuration allows fine-tuning of reaction conditions, offering flexibility to control the polymer conversion process.

Previous research has shown that steam cracking using DFB technology could process a wide range of solid waste streams, potentially replacing conventional tubular naphtha-based steam crackers for monomer production in existing petrochemical facilities [15]. Typical product species include a nitrogen-free stream of syngas, CO_2, ethylene, propylene, BTXS (benzene, toluene, xylenes, and styrene), along with some other fractions of aliphatics, polyaromatics, and char. In a 100 % carbon recycling scheme, various routes can be used to recover the carbon atoms based on thermodynamic efficiency and ease of implementation at the process downstream. The simplest route involves direct collection of monomers and valuable monoaromatics through fractionation, as these molecules can be readily used in existing synthetic material production. Methane and syngas can be repurposed next for hydrocarbon synthesis, while the nitrogen-free CO_2 can be combined with hydrogen from electrolysis for further chemical synthesis. Remaining hydrocarbons can be combusted to produce CO_2, which can be captured via CCU methods and added to the CO_2 stream for utilization.

Research on the steam cracking process in fluidized beds has been maturing over the last decade as a method for processing different types of polymer waste, with several experimental tests now reaching the semi-industrial scale [15–17]. In the case of textiles, laboratory-scale studies have explored steam cracking in both fluidized and fixed-bed reactors (also known as fixed-bed pyrolyzers under a steam atmosphere). These tests involved pure fiber types, such as PET and cotton [18,19], as well as blends with polyolefins, to evaluate the effects on the product yield [20]. At a larger scale, experiments using household textile waste were conducted in a dual fluidized bed steam cracker reactor at the semi-industrial scale, and presented in a report by Chalmers researchers as a preliminary evaluation of key species yields [21]. These results were later used in a report to assess the economic viability of the process as a carbon recycling technology for the Nordic region, comparing it with a waste-to-energy scheme [22]. The present study builds upon such preliminary data, complemented by additional experiments using rejected post-sorting household and workwear textile waste under different reactor and feeding conditions.

From the feedstock perspective, the chemical structure of the original polymers plays an important role on the product species distribution. Specifically, the nature of the bonds determines the types of free radical fragments produced during chain-breaking events. To analyze the conversion behavior of the carbon atoms in the process, this work evaluates the experimental data through a special framework developed in a previous study [16], which classifies carbon bonds into three basis groups: carbons bonded to heteroatoms (C-X), to aromatics (C-AR), and to aliphatics (C-AL). The framework creates an intersectional space that connects feedstock structure to product species at a chemical level, based on shared characteristic structural environments. In this study, the approach enables the evaluation of product species in relation to the structural groups in the feedstock, and the assessment of the bonds' fate at the process downstream through input-to-output relational indexes. The method is particularly useful for evaluating the conversion behavior of highly heterogeneous feedstocks such as textile waste.

Given the robust characteristics of the DFB reactors for processing complex polymer mixtures, the present work evaluates the feasibility of using steam cracking in a semi-industrial dual fluidized bed reactor as an alternative route for chemical recycling of textile waste. Specifically, this research assesses the yields and distributions of valuable chemical products obtained from real textile waste streams processed by steam cracking at a semi-industrial scale, aiming to evaluate the potential for carbon recovery from such wastes. Particular focus is given to the impacts of the polymeric feedstock composition on the product species from a carbon conversion yield perspective. The study examines correlations between characteristic carbon bonds in the feedstock chemical structure and the resulting species distribution, providing insights into the conversion behavior of feedstocks with high oxygen content, such as textiles. Finally, this research highlights the potential of steam cracking as an alternative closed-loop carbon recycling technology for textile waste within the context of current recycling scheme and synthetic materials production.

2. Experimental setup and methods

The experiments were conducted in the DFB cracking reactor at the Chalmers' Power Central facility. The reactor is coupled with a 12-MW circulating fluidized bed combustor operated with wood chips, using silica sand as the bed material. The fuel flow to the combustor is between 2000–2500 kg/h. The 2–4-MW cracking reactor is fluidized with steam in a bubbling regime and operates within a temperature range of 730°–815 °C to create the steam cracking conditions (Fig. 2).

Feedstock feeding to the cracker was performed at the cracker fuel input point (position 8 in Fig. 2) in the form of pellets, impelled by a couple of rotary valves in series, which function as an airlock system [23], with a rate of ~115–120 kg/h (see Table 2). To obtain a more-stable feeding rate, the feeding in the second half of the experimental set was performed with an alternative extrusion-based feeding system. The extruder feeds at the top of loop seal 1 exit at a rate between ~35–50 kg/h (position 6 in Fig. 2) and the material enter semi-melted to the reactor, ensuring no leakage of air into the system. In general, Fuel addition into the reactor presented challenges due to the light-weight nature of the pelletized feedstock, which caused some instability in the fuel flow as it dropped over the bed. It is important to note that the stability requirements for fuel feeding in this experimental setup were particularly strict to ensure precise characterization of product species and maintain low variability in carbon yield evaluation. To ensure statistically valid product species data, the characterization was performed over a period of approximate 30–60 min of uninterrupted operation for each reactor condition. During this time, the stability of the averaged species yields was continuously monitored, with relative variations kept within 10 %. During the operation, stable conditions in the combustor side are obtained as well.

The product species were characterized by extracting a sample gas stream from the reactor's outlet (Fig. 2). The sample stream passed through a hot filter for particle removal and was then split into two streams. One stream was directed to permanent gas and condensable species characterization, while the other was used for total carbon evaluation. The first stream passed through a quench loop that

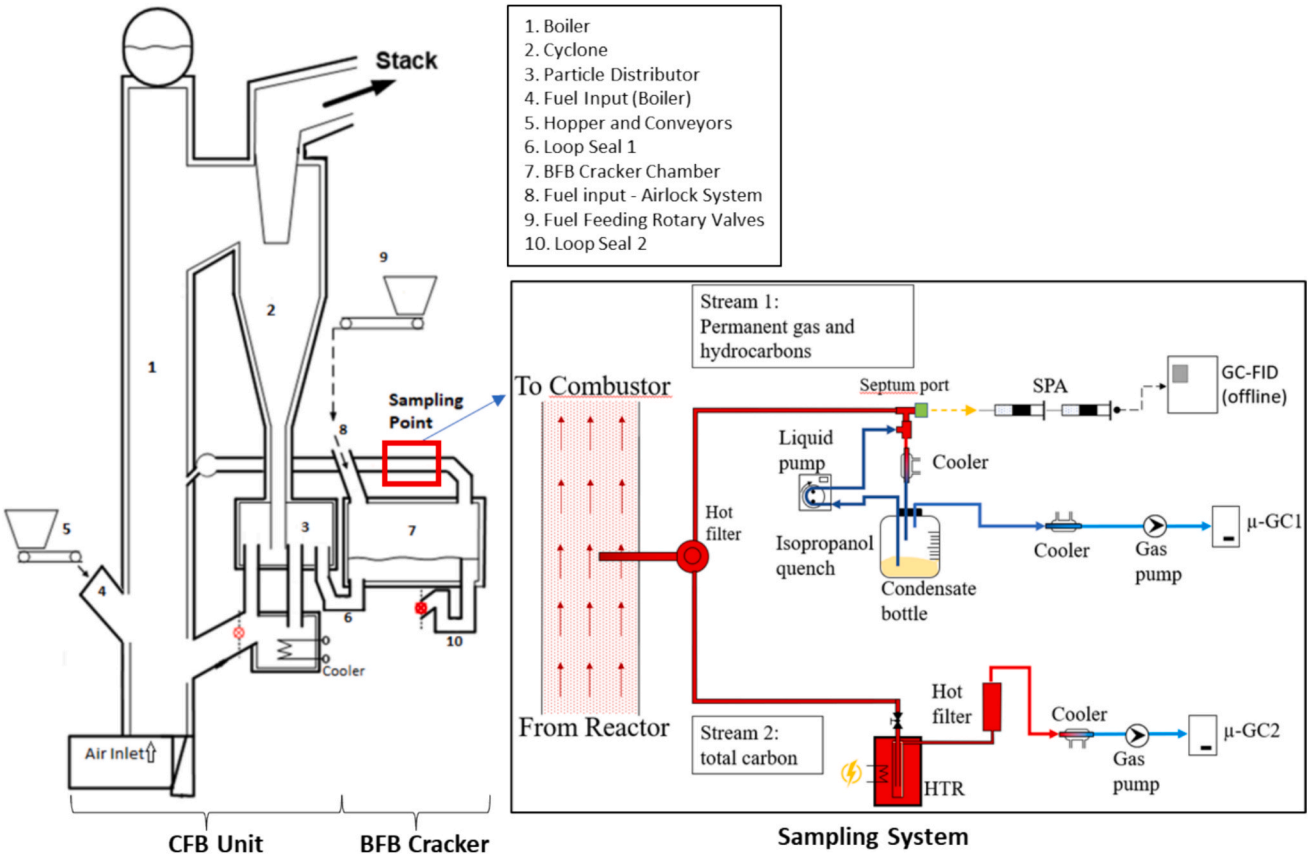

Fig. 2. Schematic of the Chalmers DFB reactor and sampling system setup (modified from [24]).

contained cooled isopropanol, to remove aromatics and long-hydrocarbon-chain species. The stream was cooled further to eliminate the remaining water. The purpose of the quenching loop and water removal is to create a dried stream containing permanent gases for on-line characterization. The dried stream was pumped up into a Varian CP4900 micro-gas chromatographer (micro-GC) equipped with a thermal conductivity detector (GC1 in Fig. 2), periodically calibrated to analyze He, H_2, N_2, O_2, and C_1–C_3 species. The stability of the whole process is monitored and quantified via chromatograms taken every 3 min from the sampling system in GC1 and an online NDIR instrument (Rosemount MLT, not shown in figure), connected in parallel to GC1, to further check the concentrations of CO, CO_2 and CH_4 from the dried gas each second. A constant flow of helium was mixed with the fluidization steam as a tracer gas for internal standard quantification in the GC.

Before the isopropanol quenching loop, a sample was extracted from the original stream for the characterization of aromatics using a Solid Phase Adsorption (SPA) method. This method involved passing 100 mL of the raw gases through an adsorbent column that consisted of a layer of amine-bonded silica, followed by an activated carbon layer (Supelclean ENVI-Carb/NH_2 SPE columns). Thereafter, the species retained in the column were eluted into a vial with a mixture of dichloromethane, isopropanol, and acetonitrile (8:1:1 ratio), and the obtained liquid was analyzed in a GC coupled with a Flame Ionization Detector (GC-FID). Two columns in series were used to ensure complete adsorption of aromatics [25], and four to five samples were collected per operative condition for statistical purposes. The SPA method was chosen because it has been proven as a fast and reliable characterization method of the condensable fraction in this system, covering species with boiling points ranging from benzene to coronene, as shown extensively in previous research [26–29]. Furthermore, as shown by Mandviwala et. al. [29], the combination of permanent gas characterization via GC-TCD, GC-FID analysis from SPA, and the High Temperature Reactor (described later) enables near-complete carbon balance closure for steam cracking of plastics, identifying and quantifying nearly 90 % of the carbon in the produced hydrocarbon species. Detailed information regarding the full characterization and sampling methods are available elsewhere [25,26].

The second sampling stream passes through a High Temperature Reactor (HTR) set to 1700 °C where the hydrocarbons are fully reformed by reacting with the steam present in the flow to produce syngas and CO_2. These gases are dried in a series of condensers before being pumped to a second gas chromatograph coupled also with a TCD detector (GC2 in Fig. 2) for further characterization of the same species as GC1. The extent of the reforming process is monitored by the yield of methane, which is expected to be zero under normal operative conditions. Additional details about this setup can be found elsewhere [30]. Since this second stream is measured in parallel with the first, the quantification of the carbon species obtained out of the HTR reactor will provide the measure of the total carbon extracted in the original sampling gas. Due to the inherent design of the dual fluidized bed (DFB) reactor, the char produced circulates continuously toward the combustor chamber. Thus, no direct char extraction or characterization was performed in this study.

The solution of the carbon balance from the reaction system based on the characterization setup is depicted in Fig. 3. Notice that the C4+ species are measured by difference between the results obtained from HTR and GC1 plus the condensable fraction from SPA.

Given the difficulties obtained in the feedstock feed, indirect measurements from TGA and tests in a laboratory scale fluidized bed (setup details in [25]) were performed, to crosscheck and validate the char yield obtained from the HTR.

2.1. Feedstock compositions and reactor conditions

Three different batches of rejected textile fractions were utilized as

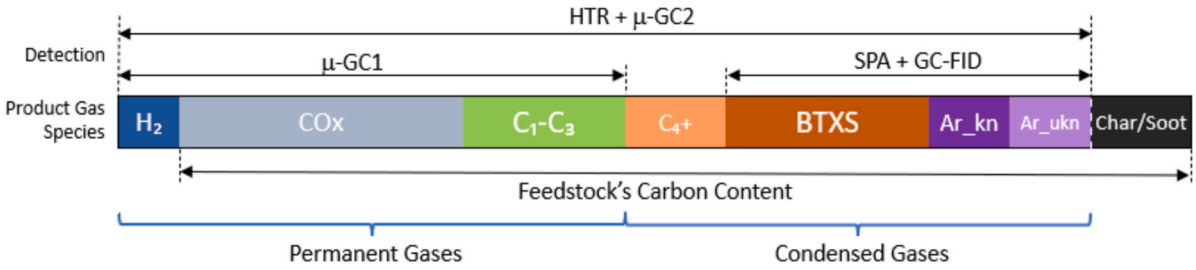

Fig. 3. Carbon Balance estimation from the implemented characterization setup (modified from [16]). AR_kn refers to other known aromatics (e.g. polyaromatics) whereas Ar_ukn refers to other unknown aromatics also identified by GC-FID from the SPA elution.

feedstocks in the experiments conducted in this work. Two of these batches were sourced from textiles collected by a charity foundation after filtering out good-quality clothes that could be resold in the country's second-hand market, as well as garments made entirely of cotton fiber. Afterwards, manual sorting was performed to remove metal objects and buttons to the greatest extent possible. In general, the waste comprised mainly by clothes, with a small fraction of home textiles, such as curtains, pillows, and blankets. Both batches originated from the waste accumulated over a certain amount of time during different months of the year. The third batch consisted of discarded common workwear supplied by the producer of such garments.

All three batches were shredded separately and converted into pellets for reactor feeding after the removal in a wind-shifter of a small heavy fraction that consisted of leftover metals and other inert materials. The ultimate analyses of the three batches are presented in Table 1.

Rough estimates of the polymeric compositions of the batches were obtained through manual identification of the clothes' tags and NIR spectrometry before pelletization. However, to reduce the uncertainty related to composition, a numerical estimation was performed using a convex optimization model built on elemental balances and low heating values. Further details regarding the developed numerical model can be found in the reference [16]. The polymeric composition is presented in Fig. 4. It should be noted that even though Batch 1 and 2 were collected at different times their compositions are similar, with PET being the predominant polymer. In contrast, workwear is predominantly cellulose due to its higher cotton content.

Considering the scale of the reactor and the feedstock flow, the number of experiments conducted was based on the total amount of collected textile waste material. The temperature range tested spanned from 735 °C to 815 °C to adapt to the operating conditions allowed by the boiler. Steam flow was maintained at a sufficient rate to ensure a steam-to-fuel ratio greater than one, while keeping a bubbling fluidization regime in the cracker. The bed material was silica-sand. The reactor conditions applied to each batch are shown in Table 2. As mentioned before, stable operating conditions were kept in the cracker and the combustor during a time span of 30 to 60 min. During that time the temperature in the cracker fluctuates approximately ±2 °C, which is automatically registered each 6 s in the database. The reported value of Table 2 corresponds with the average from the respective timespan.

The feeding to the extruder was performed manually due to the fluffy characteristic of the pelletized textiles which was difficult to handle by the automatic feeder which also incorporates a digital scale sensor. Consequently, the fuel flow was instead obtained through indirect measurements based on the periodic addition of batches to the extruder's input. To validate the estimations, the final mass flow was also cross-checked with the total carbon balance derived from the gas and HTR measurements.

Table 1
Ultimate analyses of the three textile batches tested.

Element	Batch 1	Batch 2	Batch 3	Method
C %w dry	60.53	60.93	51.95	SS-EN ISO 21663:2020
H %w dry	5.17	5.54	5.95	SS-EN ISO 21663:2021
O %w dry	29.97	28.96	37.96	SS-EN ISO 21663:2022
N %w dry	2.90	3.15	1.53	SS-EN ISO 21663:2023
S %w dry	0.09	0.07	0.11	SS-EN 15408:2011
Cl %w dry	0.12	0.12	0.37	SS-EN 15408:2011
Ash %w dry	1.30	1.22	2.11	SS-EN 15403:2011
LHV (MJ/kg dry)	28.13	28.13	17.87	SS-EN ISO 21654:2021 mod.1) a)

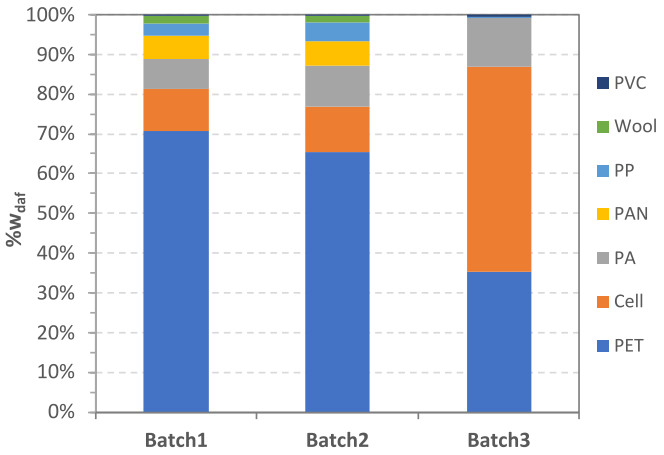

Fig. 4. Polymeric compositions of the three textile batches.

2.2. Carbon yields evaluation model

In order to evaluate the correlations between the feedstock and the products from a structural point of view, the carbon bond classification framework developed in a previous study was applied. The concept's core consists of creating an intersectional reference space that allows a comparison between feedstock and products at the chemical level, based on shared characteristic structural environments. The space consists of a generalized carbon-bond scheme that classifies the carbon bonds from the feedstock in three kinds of groups: carbons attached to heteroatoms ($C-X$), carbons attached to aromatics ($C-AR$), and carbons attached to aliphatics ($C-AL$). These groups form the basis of the framework's kernel. More details about the setting up of this framework can be found elsewhere [16]. Additionally, elemental and statistical analysis was applied to the experimental results to assess the quality of the data so the species distribution can be accurately defined [31].

For the three studied batches, Fig. 5 presents the carbon ratios for the characteristic bond groups $C-AL$, $C-AR$, and $C-_xO$ (carbons attached to oxygen by double or single bond), considering the polymeric composition shown in Fig. 4. Note that, based on the ethylene and propylene production observed in the pure PET case (Fig. 6b), the ethylene carbons in PET were classified as belonging to the C-AL group.

As shown in Fig. 5b, Batch 1 and 2 share similar carbon-bond characteristics, with the aromatics group being the most prominent, which is expected due to their predominant PET content. In contrast, Batch 3 has

Table 2
Operational conditions in the steam cracker reactor for the experiments conducted with the textile batches. (B1–3: Batch 1–3, SH: Second Hand, UF: Used Clothes Factory, RV: Rotary-valves, EX: Extruder).

Experiment	1	2	3	4	5	6	7	8	9
Batch Number	B1	B1	B2	B2	B2	B2	B2	B3	B3
Textile Waste Origin	SH	SH	SH	SH	SH	SH	SH	UF	UF
Temperature Cracker	790	815	735	790	765	810	815	756	758
Material Flow (kgdaf/h)	118	114	147	128	49	49	36	51	38
Total Steam (kg/h)	209	209	230	215	218	215	215	215	135
Feeding System	RV	RV	RV	RV	EX	EX	EX	EX	EX

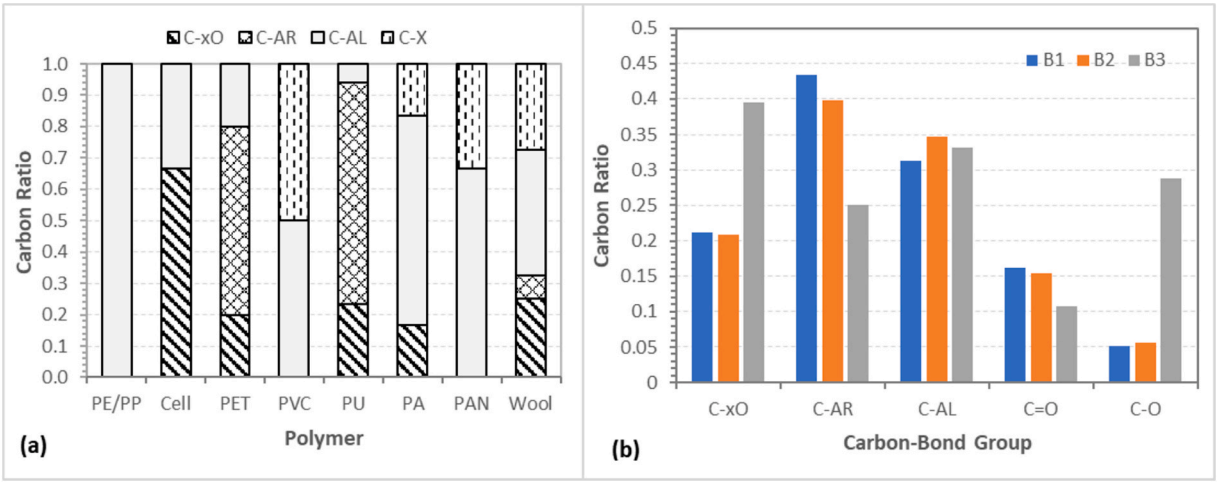

Fig. 5. Results of the carbon ratios for the three bond groups defined in the correlation framework for the three batches analyzed, for the pure polymers panel (a), and for the evaluated feedstock's batches (panel b).

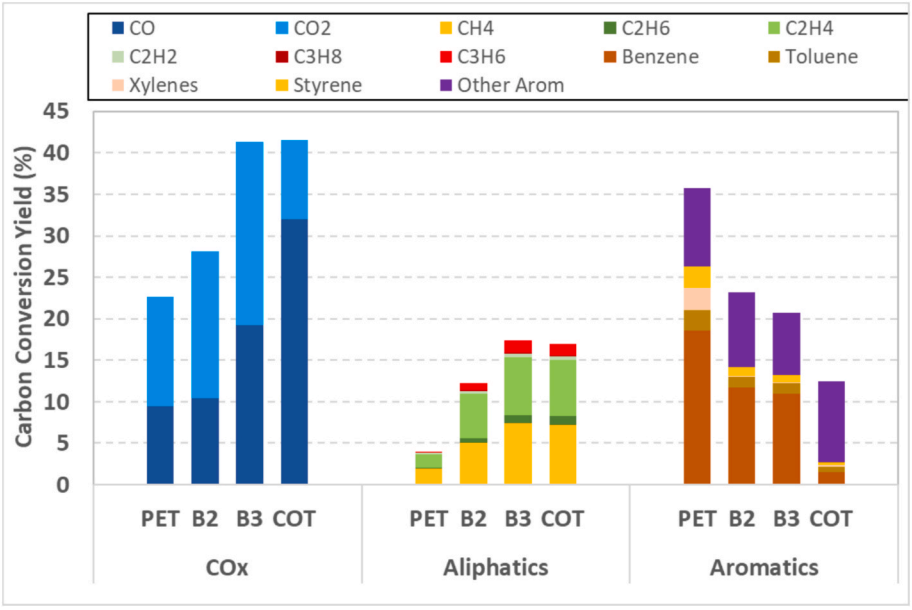

Fig. 6. Results of the percentage of carbon from the feedstock converted into the measured species for the evaluated textile batches (batch 2 and 3) under similar temperature conditions (~760 °C). The figure includes the results of pure PET and cotton obtained from lab scale tests as reference.

a higher proportion of carbons attached to oxygen, primarily from the ether and hydroxyl linkages in the cellulose from cotton. The share of carbons attached to aliphatics is relatively similar across all batches.

In this work, to assess the conversion of the carbon to the species with respect to the feedstock's chemical structure scheme the carbon conversion index (*CI*) is employed. Here, the conversion index is defined as the ratio between the evaluated specie (or group of species) and the corresponding carbon-bond group in the feedstock, as presented in Fig. 5b. This index is bounded within the domain $CI_j \in [0, 1/r_j]$ where j represents the carbon bond group, and r its respective carbon ratio in the feedstock. A CI_j value of 0 indicates that all carbons from bond group j have been converted into other kinds of product species. Contrarily, an index of $CI_j = 1/r_j$ indicates that all carbons in the feedstock have been

converted into the product species evaluated by that index. An index of 1 corresponds to the special case where the evaluated product species can be seen in a form of "equilibrium" with the respective feedstock's carbon-bond group (bonds inflow = bonds outflow).

3. Results and analysis

3.1. Overall cracking species yields

This section presents an overview of the cracking product species in terms of their carbon share in order to assess the conversion behavior of the textile waste batches relative to the respective feedstock's carbon content. Fig. 6 shows the percentage of carbon from the feedstock converted into the measured species (denominated hereby as carbon conversion yield) for the batches 2 and 3 at a similar reactor temperature (760 °C ± 5 °C). There is no available data at the chosen temperature for Batch 1, but since its composition.is similar to Batch 2 (see Fig. 4), it is expected to display a similar behavior (as will be detailed in the Section 3.2). The figure also includes the species conversion yields of pure PET and cotton obtained from lab scale for reference purposes. More details of the yields obtained from all the experiments conducted on the three textile batches can be found in the Appendix in Table A 1 and Fig. A 1. Note that the statistical uncertainty of the results presented is between 3 % and 7 % for all the evaluated cases.

As it can be seen in Fig. 6, the relative distributions of syngas, aliphatics, and aromatics in the product gas follow a similar pattern for the evaluated batches, i.e., the syngas (H_2 and CO) plus CO_2 contain the largest share, followed by the aromatic species and then the aliphatics with the lowest share. Among all measured species, CO_2 has the largest share spanning from 18 % to 22 % for the tested batches. Syngas production shows large variation relative to the batch type, with carbon conversion yields of 10 % and 19 %, for Batch 2 and 3 with the highest level observed for Batch 3. This significant share of carbon oxides in the product gas correlates directly with the large oxygen content of the PET and cellulose chemical structures present in the feedstock. This is a common behavior observed for all batches across all tests (see Fig. A 1 of Appendix). The difference in CO production between the results for Batch 2 and 3 suggests a stronger influence of the cellulose on the production of such specie, since Batch 3 contains a larger cotton content (see Fig. 4). This result suggests that the ether-like groups in the monosaccharide structure of cellulose, are more susceptible to be released as CO. On the other hand, Batch 2 is more PET-based, and it presented a larger share of CO_2 which can be related to the presence of carboxyl groups in the ester linkages of PET, This behavior is corroborated by the reference results of pure PET and cotton (COT) which show a larger share of CO_2 for PET whereas the CO yield rate was larger for cotton. The obtained yields of CO and CO_2 from the evaluated textile wastes align well with those previously reported for other oxygen-rich polymeric wastes processed under comparable steam cracking conditions [15,16]. For instance, recycled cardboard and automotive shredder residues exhibited carbon conversions to CO_x species around 25 % and 30 % on average respectively, which further illustrate the important role of chemical structure in the product species distribution, particularly when oxygenated functional groups are present.

The measured aliphatic species from C_1 to C_3 in Fig. 6 showed conversion yields of 12 % and 17 % for Batch 2 and 3 respectively. Ethylene and Methane take around 85 % of the of the measured aliphatics share. The ethylene yield rate is around 5.5 % and 7 % for batch 2 and 3 respectively and followed by a similar rate of methane corresponding with 5 % and 7 % for the same mentioned batches. In general, the yield rates of the aliphatics group is expected to be low compared with the rates of polyolefin- based feedstocks (rates of 60 % to 70 %, see [17,29]). This is an expected outcome due to the small share of polyolefins in the feedstock's composition and also agree with the reference PET and cotton values which set a range between 4 % and 17 % for the aliphatics species.

Regarding the aromatics fractions, Fig. 6 shows similar yields for Batches 2 and 3, with respective yield rates of 14 % and 13 % for BTXS (Benzene, Toluene, Xylenes, Styrene) and 9 % and 7 % for other aromatics. The reference results displayed in Fig. 6, present PET as the more relevant in terms of aromatics production, which suggests this polymer's protagonist role in the aromatic yields of the textile wastes. The rest 36 % and 20 % of the carbon fraction for Batch 2 and 3 respectively, correspond to char and other C4 + unknown aliphatics.

3.2. Carbon conversion evaluation

Fig. 7 shows the percentage of carbon conversion from the feedstock into syngas, CO_2, light olefins, and valuable aromatics (BTXS) after the cracking process. The figure also includes results from tests with pure polyethylene (PE) under similar conditions in the large reactor, as well as laboratory-scale experiments using pure PET and cotton, for reference purposes. Note that in this case, "syngas" refers only to the CO results. Batch 1 (B1) is represented by empty circles, Batch 2 (B2) with filled circles, and Batch 3 (B3) with triangles in all panels. For reference, the squares represent lab results for pure Cotton (yellow) and PET (grey). For ease of reading, panel b only shows ethylene results for lab scale datasets while for panel d only the BTXS results.

From Fig. 7a, it is evident that Batch 3 has the highest CO levels among all tests, reaching up to 19 % of carbon conversion yield. This is likely due to the higher cellulose content in the batch, which provides oxygen in the form of C-O bonds from hydroxyl and ether groups. Batch 2 shows a moderate increase in CO levels as temperature rises, with carbon conversion ranging from approximately 8 % to 11 %. As expected, Batch 1 follows a similar trend to Batch 2, given their comparable compositions. In contrast, CO_2 levels, as shown in Fig. 7c, are significantly higher for all batches compared to their respective CO levels. Batch 2, in particular, exhibits a sharp increase, with carbon conversion yield rising from 15 % to 30 %. These differences between CO and CO_2 trends can be explained by oxygen exchanging reactions as the water–gas shift (WGS) equilibrium, which can regulate CO levels in a steam-saturated environment. CO is initially released from the oxygen-containing polymers and is then consumed in the WGS reaction with steam, producing CO_2. The difference becomes more significant as the temperature increases, as seen by the rapid increase in CO_2 yield (see Fig. 7d). Further discussion can be found later in this section in the analysis presented for Fig. 8a. It is important to know that other oxygenated species such as acids, alcohols and others, accounted for less than 1 % of the total carbon for all the evaluated conditions, which is insignificant in comparison with the CO_x species yields, and therefore they will not be taken into account in the subsequent analysis.

Regarding the olefins production, a mild decreasing trend is observed in Fig. 7b for the conversion yields of ethylene and propylene, reaching apparent stable levels at approximately 5.5 % and 0.7 %, respectively, after ~760 °C for all batches. For BTXS, the results for Batches 1 and 2 in Fig. 5d show also a mild increasing conversion trend with increasing temperature. For Batch 3, the average conversion yield was somewhat similar than Batch 2 at similar temperature. In general, the olefins and aromatics yield rates behaviors for the batches can be attributed to specific chemical structural characteristics of the polymer composition, which will be discussed further later in this section.

It is important to highlight that for Batch 3 there is a noticeable gap between the results of the two tests for the species shown in Fig. 7, particularly for CO and CO_2, even though both tests have similar temperatures. Specifically, the CO level in the first test is higher than in the second (Fig. 7a), whereas the CO_2 level is higher in the second test, with essentially the same gap's magnitude. This behavior may be attributed to the difference in steam flow between the two tests, which directly impacts the residence time of the gases in the reactor. When the steam flow is reduced, the residence time increases, allowing the water–gas shift (WGS) reaction to have a prolonged impact on the CO conversion, which tends to equimolarly convert into CO_2 in the steam-saturated

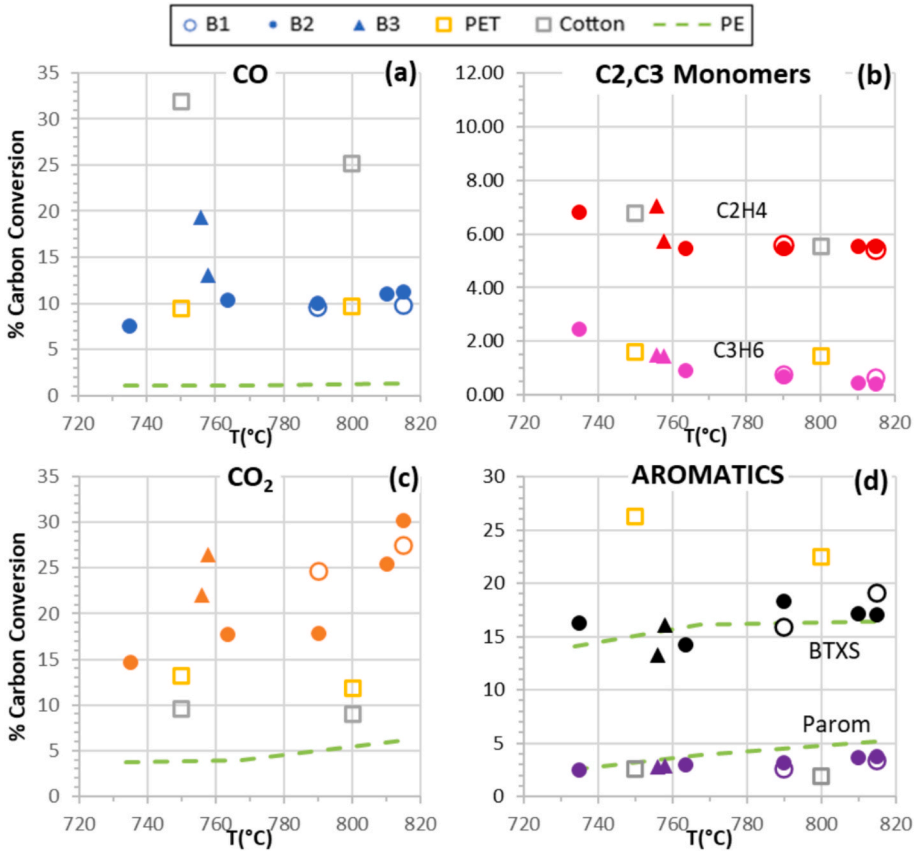

Fig. 7. Carbon conversion behaviors of key species with respect to the reactor's temperature: a) syngas (CO in this case); b) ethylene and propylene; c) CO_2; d) BTXS and identified Polyaromatics. The green dotted line represents the pure polyethylene case. (the yield rates for PE in panel b are at around 30% for ethylene and 13% for propylene, which are out of the chart range). (For interpretation of the references to colour in this figure legend, the reader is referred to the web version of this article.)

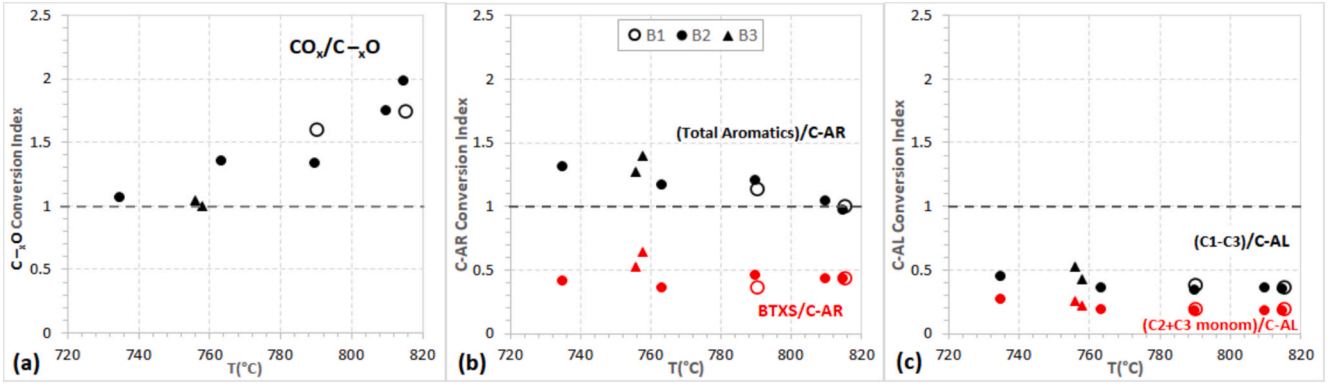

Fig. 8. Carbon conversion index of COx (Panel a), aromatics (Panel b) and aliphatics (Panel c) species based on their related feedstock's carbon-bond groups. In all panels, Batch 1 (B1) is represented by empty circles, Batch 2 (B2) with filled circles, and Batch 3 (B3) with triangles. Total aromatics include the char fraction.

environment (this shift is also clearly seen when comparing the carbon conversion index of CO_2 and CO in Fig. 9). Now, for the gap observed in the olefins and BTXS cases, in addition to the increase of residence time, a reduced steam flow results in less dilution of the nascent volatiles from the moment the polymer chains start to breakdown. This increases the likelihood of recombination reactions between radical chains, with cyclization reactions being particularly significant. These reactions lead to the aromatization of previously aliphatic structures, as seen in the polyethylene cracking yields (see Fig. 7d), and involve key ring precursors like ethylene and acetylene [25,32].

Overall, the observed conversion ratios for the tested textile batches are consistent with the relative behaviors observed in lab-scale experiments using pure cotton and PET. In the lab tests, cotton showed higher carbon conversion yield for all species displayed in Fig. 7, especially for CO (Fig. 7a). However, CO_2 levels were relatively low in the lab tests, likely due to shorter residence times at this scale, which limited the extent of the WGS reaction and the subsequent conversion of CO into CO_2, as explained before.

When comparing the textile results to the PE reference (green line in Fig. 7), the CO and CO_2 conversion yields were significantly higher for the textile batches, as expected due to their higher oxygen content. In contrast, the conversion yields of ethylene and propylene were much

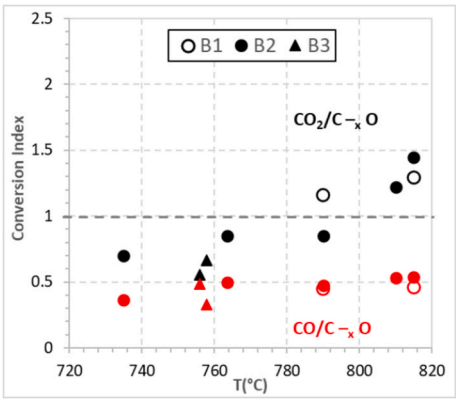

Fig. 9. Carbon conversion index of the total carbon attached to oxygen bonds for CO2 and CO in the three analyzed batches.

lower for the textiles, since PE exhibited conversion yields of around 30 % for ethylene and 13 % for propylene as a result of its polyolefinic chain structure. Notably, the BTXS conversion in Fig. 5d was almost identical for both PE and textiles, particularly the PET-based batches (B1 and B2). This is a noteworthy result, considering the different formation mechanisms for both materials. In the textiles, the aromatic rings present in the structure are mainly released as aryl radicals, which can condense directly into monoaromatics. By contrast, PE, which lacks aromatics, forms the rings through cyclization reactions obtained from aliphatic radical recombinations. An additional mechanism of cyclization may occur in the textiles by the presence of chlorine attached to carbons in the polymer chain. The high electronegativity of chlorine affects the electron density making the bond susceptible to breakage during a free-radical event. Released chlorine from alkyl chains tend to remove a neighbor hydrogen to form hydrochloride, leaving behind reactive sites that can form conjugated dienes which are cyclization precursors for aromatic or polyaromatic structures [33]. However, given the small share of chlorine reported in the elemental analysis (Table 1), it is not expected to have a significant aromatization effect through this route.

3.2.1. Carbon conversion index

Based on the method presented in Section 2.2, to assess the carbon conversion yields with respect to the feedstock's chemical structure, Fig. 8 displays the carbon conversion index (*CI*) versus temperature of the characteristic product species groups, i.e., CO_x, total aromatics (char included) and aliphatics, evaluated for the three studied batches. To further analyze the CO_x species, Fig. 9 shows the conversion index of the total carbons bonded to oxygen for CO_2 ($CO_2/C{-_x}O$) and for CO ($CO/C{-_x}O$).

From Fig. 8a, it is possible to observe that the conversion index for $C{-_x}O$ presents a positive trend as temperature increases. The index is larger than one in a large portion of the temperature range, which can be seen as an indication of reforming reactions occurring in the process, where aliphatic or aromatic species are being transformed into CO_x due to the saturated steam environment. This effect becomes more pronounced as the temperature rises.

For the lower temperature cases, the reforming effect in batch 2 seems less significant, as the index is close to one. This indicates that the CO_x species produced are roughly balanced out with the oxygen content in the feedstock's structure, meaning that no external oxygen sources are significantly impacting the ratio of $C{-_x}O$ bonds to CO_x species. This behavior is more clearly illustrated in Fig. 9, which shows the conversion index of $C{-_x}O$ for CO_2 and CO. At lower temperatures, both indices are less than one, but their sum is equal or greater than one. This suggests that external oxygen to the structure is not yet participating significantly in the CO and CO_2 formation. As temperature increases, the CO index shows a slight increase whereas CO_2 index increases faster even surpassing the $CI = 1$ level. This implies that carbon from other groups, along with steam, are being converted into CO and then transformed into CO_2 through the WGS reaction or the natural bed's oxygen transport due to metal oxides in the sand as shown in previous research [25,31,34].

In contrast, Fig. 8b shows that the C-AR conversion index for total aromatics is larger than one at the lowest temperature (~735 °C) and follows a decreasing trend as temperature rises, until reaching a level around one at ~815 °C. In this case, an index above one can be seen as an indication of new aromatic structures formation, likely through cyclization reactions from aliphatics, whose conversion index remains below one across all temperatures (see Fig. 8c). Meanwhile, the index for the monoaromatics (BTXS) remains relatively stable and below one throughout the temperature range, suggesting that the new aromatics formation involves also the radical rings of the feedstock's structure and progresses towards the synthesis of polyaromatics and char.

The rapid decrease in the total aromatics index, relative to the nearly stable aliphatics and BTXS indices even at higher temperatures, suggests a direct correlation with the sharp rise in the CO_x index. This implies that most of the CO_x species might come mainly from the reforming of their aliphatic precursors, such as C_2 radicals and possible C_1 also, similar to the mechanism observed for CO_x formation during PE gasification (see Fig. 7a,c).

Overall, higher temperatures seem to favor reforming reactions to produce CO_x species while maintaining relatively stable conversion into valuable chemicals, such as BTXS and C_2-C_3 monomers. Conversely, as temperature decreases the conversion to CO_2 decreases, suggesting that hydrocarbon oxidation is less active in the system at temperatures below 760 °C, which favor the survival of precursors that participate in high order cyclization resulting in increased production of complex structures as polyaromatics and char. Additionally, PET and cellulose are among the most oxygen-rich polymers that can be found in waste streams, with a relatively low aliphatic carbon content. The results presented in Fig. 8 may thus serve as a useful reference for a limit case scenario in evaluating the conversion index, particularly for CO_x and aliphatics, when considering other types of mixed polymeric streams under similar reactor conditions.

3.3. Recycling potential assessment

Due to their origin, Batches 1 and 2 may serve as representative examples of a typical household textile waste stream, which, as noted in Section 1, comprise about 85 % of the total textile waste. Accordingly, Fig. 10 summarizes the mass yields of valuable species for the average of Batches 1 and 2. Here, the "daf" subscript indicates on a dried and ash-free fuel basis. It is important to note that due to the low ash content, the difference between the feedstock mass on a dried basis and expressed as daf is practically negligible.

Based on the results shown in Fig. 10, the share of valuable chemicals (C_2 + C_3 monomers + BTXS) retrieved from the steam-cracking of household textile waste ranges from 14 $\%wt_{daf}$ to 18 $\%wt_{daf}$ for the evaluated temperatures. As mentioned previously (Section 1), these fractions can be recovered directly out of a fractionation process. Syngas and methane, which are considered part of the valuable gases fraction in the energy sector, account for an additional 16 to 22 $\%wt_{daf}$. These yields correspond to an average carbon conversion yield of 24 %C to valuable chemicals and of 16 %C to valuable gases (syngas plus CH_4), relative to the feedstock's carbon content under the evaluated cracking conditions. Overall, the observed variations in the yields of valuable species as the temperature rises in the evaluated range are relatively small, which underlines the constraint imposed by the characteristic feedstock's chemical structure on the types of species produced.

Based on the concept mentioned in the introduction of repurposing methane and syngas for chemical synthesis as a secondary route, the syngas generated from the process has an averaged H_2/CO molar ratio ranging from 1.02 to 1.93 for the low and high temperature cases (See

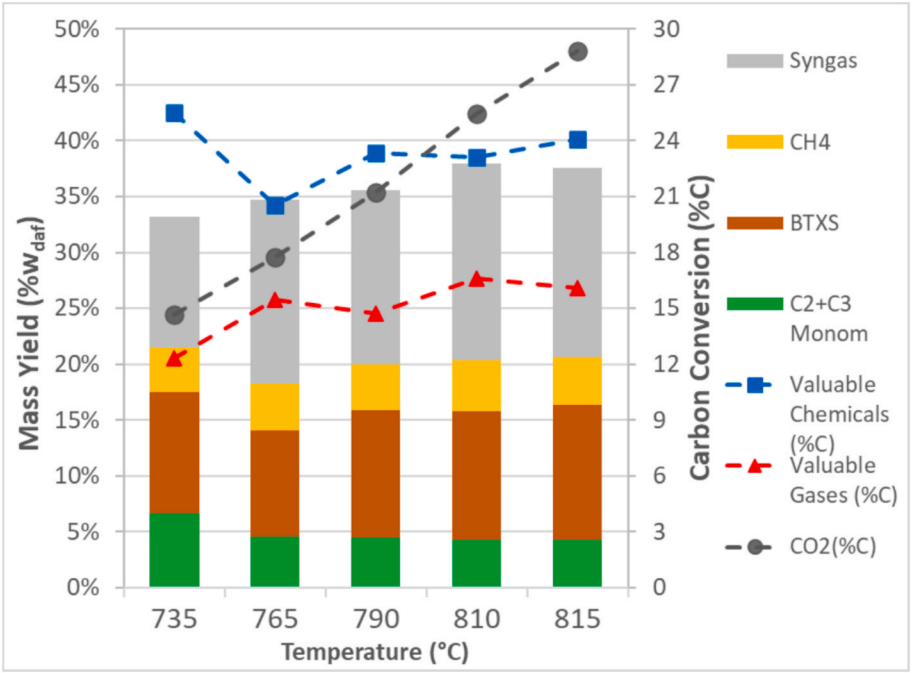

Fig. 10. Yields of valuable species obtained from Batches 1 and 2. Left axis: Mass yield in %w_{daf}, applies for column bars. Right axis: Carbon conversion percentage (%C), applies for dotted lines. Valuable Gases: Syngas + CH4; Valuable Chemicals: C_2,C_3 Monomers + BTXS.

Table A 1). Such level is low compared with the H_2/CO ratio of 2 required for Fischer-Tropsch synthesis of hydrocarbons. For methanol synthesis, which is a valuable chemical for the materials and chemicals industry [35–37], the ratio in practice may go up to 3.5 in industrial settings [38–40]. To meet the minimum required 2:1 ratio for synthesis, additional hydrogen would be needed; approximately 1 kg/ton$_{daf}$ up to 8 kg/ton$_{daf}$ for the high and low temperature cases. This hydrogen could be supplied via steam reforming of the produced methane (SMR), which would generate around 5 to 6 kg/ton$_{daf}$ of hydrogen surplus, or via electrolysis from renewable sources (electricity demand of 50–400 kwh/ton$_{daf}$, based on a standard electrolysis consumption of 50 kwh/kg$_{H2}$ [41,42]).

After the downstream separation, the third route for carbon to chemicals recovery implies the use of the obtained nitrogen-free CO_2 stream for synthesis, which require a higher hydrogen input than in the syngas case. The minimum hydrogen required for CO_2 synthesis is a 3:1 H_2/CO_2 ratio, which translates to approximately 45 to 90 kg/ton$_{daf}$ of hydrogen, which can be supplied also by electrolysis with the subsequent increase in the energy demand (2.3–4.5 Mwh/ton$_{daf}$). In terms of yields, CO_2 has a significant variation as temperature increases while the valuable species sets remain relatively stable (see Fig. 10). Thus, from a technical perspective it may be convenient to pick the high temperature cases (>790 °C) since the clean CO_2 stream recovery can add up till 29 % of the carbon with minimum effect on the valuable species yields.

Finally, the left-over fraction constituting around 31 % of the carbon, which include high order aromatics, char and other molecules larger than C_4, can be combusted to produce CO_2 and recovered fully via carbon capture (CC) methods or up till 90 % of the CO_2 with reasonable efforts [43,44]. This stream will require at most ~96 kg/ton$_{daf}$ of additional hydrogen. The resulting energy can be used to power the steam-cracking process. While the costs for implementing such approach are high, especially if the carbon capture unit must be built, it remains still an option for a full circular carbon economy under the carbon capture and utilization (CCU) context [45], but with a smaller CC unit than if all the textile waste would be fully combusted.

In the context of the European textile recycling situation [2] currently only 3 % of the carbon from the collected textile waste fraction is recycled in closed-loop form through mechanical methods (See Fig. 1, the weight percentages can be taken interchangeably to carbon percentages within a low margin of variation assuming homogenous mixtures, the approximation holds as long as the highly selected fraction −closed-loop fraction- be relatively low, which is this case). Approximately 30 % of the collected fraction goes to open-loop processes while the remaining ~67 % is destined for reuse (Fig. 1), but in reality, most of it is exported, likely ending up in uncontrolled landfills or incinerators [3,46]. Moreover, there are costs associated with sorting and handling at each stage of this recycling scheme [2,5]. Also, general public's preconceptions and complex sorting guidelines create a quality bias that make people set arbitrary standards to decide which garments are worthy to be disposed of in the recycling sites, discarding the rest as common waste [47,48].

In comparison to steam cracking of polyolefin-based feedstocks, which achieve carbon conversion yields of 40 % to 60 % [17,29], the direct carbon conversion yield into valuable chemicals is relatively low for textile wastes. However, given today's recycling situation, and the fact that all selective, material specific, recycling methods leave a sorting residue, steam cracking might offer an opportunity for not only a substantial carbon recovery improvement but also to reduce complexity of the recycling guidelines transmitted to the public. Considering a recycling scheme within the broader framework of the synthetic chemicals and materials production system, the collected waste fraction can be directly allocated to the recovery of chemicals via steam cracking. Such ideal route would have the potential to increase the share of closed-loop recycling up to 24 % of the carbon, without the need for complex presorting. Moreover, if the syngas fraction is used for chemical synthesis, with hydrogen supplied via electrolysis and SMR, this recycling share could be further increased up to 40 %C, and even up to 69 % if the CO_2 stream out from the cracker is also considered in the synthesis (see Fig. 11).

In terms of heteroatoms emissions, large presence of chlorine in textile wastes may lead to the release of significant amounts of HCl as mentioned before. Additionally, organic chlorinated compounds might be formed such as polychlorinated dibenzo-p-dioxins and dibenzofurans (PCDD/Fs) as shown in previous research [49]. The presence of chlorine may influence catalyst deactivation in downstream processes and HCl in the gaseous phase can contribute to corrosion in industrial reactors,

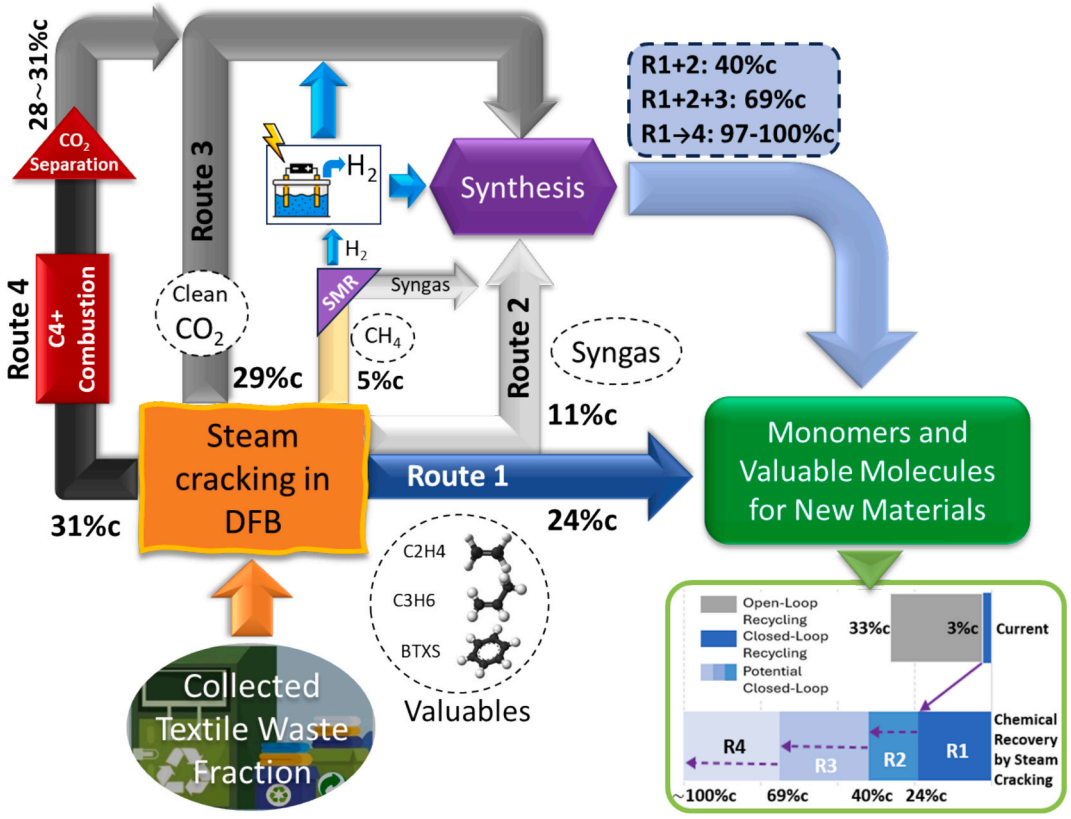

Fig. 11. Schematic of potential carbon flows of textile recycling via Steam Cracking (R = route, %c: carbon conversion yield).

particularly at high temperatures, and may require neutralization or special mitigation strategies [50]. Similarly, sulfur in the textile waste can lead to the formation of sulfur oxides (SO_2 and SO_3), which are known precursors to acid rain and can also contribute to catalyst poisoning in certain downstream applications [51]. These challenges present several avenues for future research to enhance the viability of textile waste valorization through steam cracking.

Overall, as demonstrated by the results of the present work and in previous studies with other materials [16], steam cracking in DFB is a robust technology for processing heterogeneous polymeric mixtures, such as those found in textile wastes, without the need for complex presorting. Moreover, economic cost estimations have shown that textile waste recycling via steam cracking for chemical recovery and methanol production may be an economical viable alternative depending on the reactor scale and the methanol price. For a stand-alone plant of 500kton/year capacity, the costs are estimated between ~0.8 and 0.2 EUR/$kg_{textiles}$ in a 100EUR/MWh electricity price scenario to satisfy the process' hydrogen demand [22]. Viewing it in context, a piece of cloth may weigh on average ~500 g, then, the recycling cost would be at most 0.4 EUR per piece of garment, which can easily be assumed by the consumer side. The implementation of this technology in existing chemical cluster can create a direct synergy that allows to include textile waste as an alternative feedstock alongside other polymeric materials. In such a scenario, existing fractionation and distillation units can be used with some product gas precleaning, which may reduce the investment cost between 20 and 50 %. Lastly, the eventual integration of this technology into a refinery process coupled with carbon capture for chemical recovery, may lead to achieve the ultimate goal of 100 % carbon recovery in the synthetic materials production chain [45]. As a final remark, the application of steam cracking for textile recycling can become economically more attractive if textiles are a minor fraction of a blend of polymeric waste of the feedstock, as the yields of valuable chemicals from processing textiles alone might be too small to justify the fractionation of the products. This is indeed a plausible reality, considering that the amount of plastic consumption in Europe is roughly an order of magnitude larger (~50–60 Mton) [52] than the amount of textiles disposed, therefore, textile waste fraction would be around 5–10 % overall. This will allow for improved fine-tunning of the conditions to maximize the valuable chemicals yield.

4. Conclusions

This study explored the potential for producing valuable chemicals from textile waste through steam cracking in a Dual Fluidized Bed (DFB) reactor. The results demonstrated the viability of this process for handling heterogeneous feedstocks, such as rejected textile waste fractions, and converting them into syngas, aromatics, and aliphatic hydrocarbons. Three batches of textile waste were tested at different cracking temperatures. Two of them coming from household rejected fraction in Sweden, characterized by a large fraction of polyester fibers, and the last one from discarded workwear clothes with a predominant share of cotton. The key finding as summarized as follows:

I. In terms of carbon conversion, CO and CO_2 showed the largest yield rates accounting for ~22 % to ~41 % of the total carbon converted from the evaluated batches across temperatures. The light olefins set, corresponding to ethylene and propylene, had stable conversion yields below 10 % while the methane yield was between ~5 % and ~7 %. For BTXS the conversion ranged between yields of 13 % to 19 %, with benzene corresponding with approximately 70 % of it.
II. In general, the chemical structure of the feedstock plays a crucial role in species distribution. Cotton-based workwear showed a higher yield of syngas in relation to the other species, whereas PET-based household clothes gave higher relative CO_2 and aromatics yields. This effect was attributed to the presence of

carboxyl and aryl groups in the PET, which can become stable radicals that are prone to end up after the cracking as CO_2 and aromatics, respectively. On the other hand, the oxygen of the hydroxyl and ether-type bonds in the cotton's particular cellulose structure is more likely to become CO, as evidenced by the higher yield of syngas from the cotton-based clothes. Although the batches evaluated in this study provided representative examples of common textile wastes, further research should explore a wider range of textile mixtures—including varying proportions of natural, synthetic, and blended fibers—to deepen the understanding of product distributions and refine operational parameters for optimal performance.

III. The carbon conversion index (CI) analysis was introduced to evaluate the conversion at the chemical level between the product distribution and feedstock composition through the definition of key chemical structural environments described by a carbon-bond based framework. As temperature increased, it was observed that the conversion of oxygenated carbons (C-O) to CO and CO_2 intensified, especially for CO_2, particularly through oxidation reactions of aromatic precursor with steam or the beds oxygen transport and the WGS equilibrium. Carbons attached to aromatic structures (C-AR) in the feedstock remain as aromatic rings, with half of them providing a relatively stable conversion yield into monoaromatic structures (BTXS). Contrarily, carbons in aliphatics (C-AL) contributed to the total aromatic conversion yield via cyclization reactions, with an indication that high temperatures may favor the conversion into CO_x over other species.

IV. Under the evaluated conditions, valuable chemicals (BTXS, C_2, and C_3 monomers) and valuable gases (syngas and CH_4) represent feasible recycling routes, achieving respective carbon conversion yields of up to ~24 % and ~16 % when paired with supplementary electrolysis hydrogen for chemical synthesis. This represents a significant improvement over the current European textile recycling scheme, which only achieves ~3 % of closed-loop recovery. Furthermore, a clean CO_2 stream is obtained as a byproduct of conversion and separation from the first two routes, offering additional carbon suitable for synthesis that could increase the total recycling rate to nearly 70 % with enough hydrogen availability. Economic assessments indicate that textile waste recycling through steam cracking could be obtained at less than €0.40 per garment, which is an affordable cost even for the consumer side. Integration of this process into existing chemical cluster or refineries could potentially unlock full circularity of the carbon flows in synthetic materials production, requiring less-extensive combined carbon capture and utilization approaches compared to full waste incineration schemes.

Overall, the steam cracking of textile waste in DFB reactors presents significant societal and environmental benefits by providing a viable chemical recycling route capable of converting challenging waste streams into valuable chemicals. The key advantages include reduced dependency on fossil-based feedstocks, effective processing of highly heterogeneous waste mixtures without extensive pre-sorting, and the potential for integration within existing refinery infrastructures to achieve high carbon recovery rates. However, challenges remain, primarily related to process optimization for varying feedstock compositions, further development of feeding strategies and mechanisms, and economic feasibility dependent on scale and market conditions. Addressing these factors through future research will enhance the technology's role in national and international efforts toward a sustainable resource management transition.

Declaration of generative AI and AI-assisted technologies in the writing process

During the preparation of this work the author(s) used Grammarly in order to improve language and readability. After using this tool/service, the author(s) reviewed and edited the content as needed and take(s) full responsibility for the content of the publication.

CRediT authorship contribution statement

Renesteban Forero-Franco: Writing – original draft, Visualization, Validation, Software, Resources, Methodology, Investigation, Formal analysis, Data curation, Conceptualization. **Isabel Cañete-Vela:** Writing – review & editing, Validation, Resources, Investigation. **Teresa Berdugo-Vilches:** Writing – review & editing, Visualization, Investigation. **Chahat Mandviwala:** Resources, Investigation. **Nidia Díaz Perez:** Resources, Investigation. **Ivan Gogolev:** Resources, Investigation. **Henrik Thunman:** Writing – review & editing, Project administration, Funding acquisition. **Martin Seemann:** Writing – review & editing, Supervision, Project administration, Funding acquisition, Conceptualization.

Declaration of competing interest

The authors declare that they have no known competing financial interests or personal relationships that could have appeared to influence the work reported in this paper.

Acknowledgments

This work was financially supported by the Stiftelsen Svensk Textilforskning (Project: Återvinning av textila/polymera material), the project framework Climate-leading Process Industry (Vinnova) (Project: Återvinning av rejektströmmar från textilsortering och kartongåtervinning), and Borealis AB, Sweden (Project number: 49514-1). The authors thank Jessica Bohwalli, Johannes Öhlin and Rustan Hvitt for technical support during the experiments.

Appendix

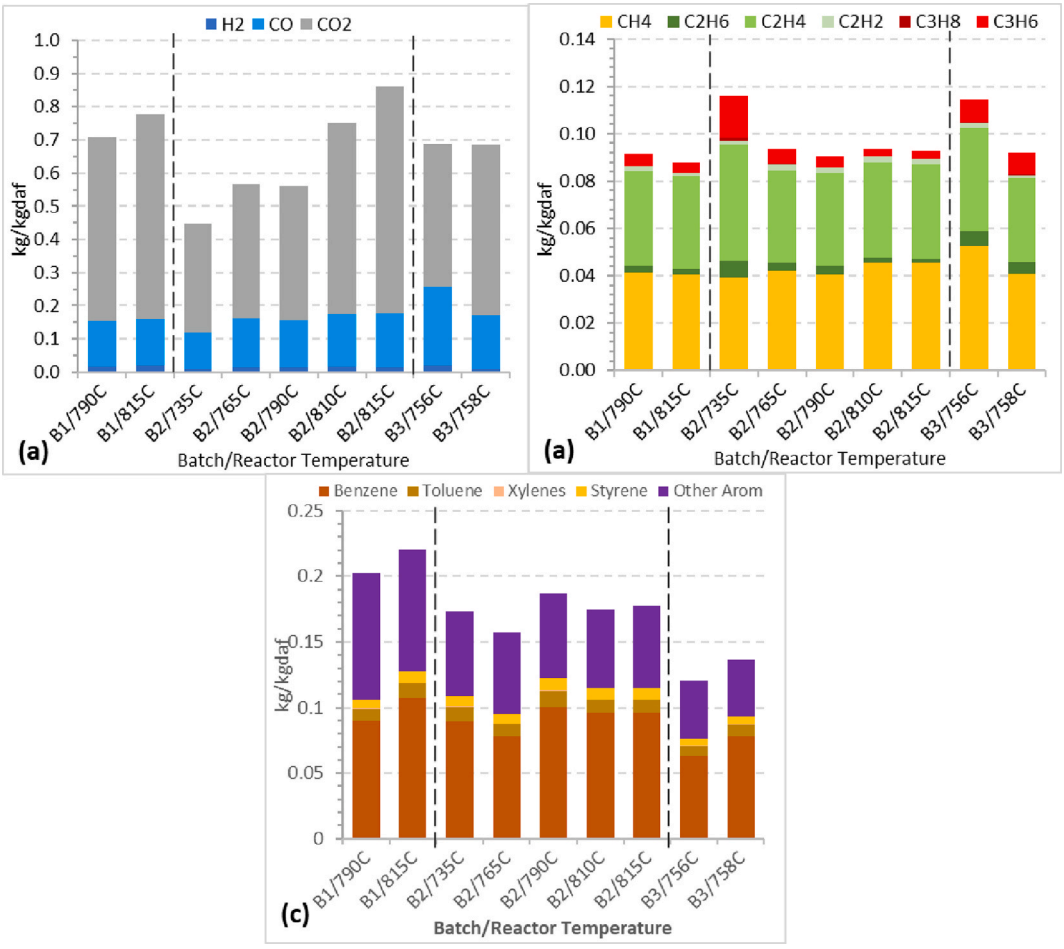

Fig. A 1. Mass yields results of the cracking experiments for the three different textile batches performed under different reactor conditions (daf, dried and ash-free fuel basis). Panel (a) shows results for H2, CO and CO2 gases. Panel (b) shows results for C1 to C3 hydrocarbon species. Panel (c) shows results for main aromatics.

Table A 1
Results of the cracking experiments for the three different textile batches performed under different reactor conditions (daf, dried and ash-free fuel basis).

Experiment	1	2	3	4	5	6	7	8	9
H_2 (kg/kg_{daf})	0.018	0.019	0.008	0.014	0.014	0.017	0.016	0.021	0.009
CH_4 (kg/kgdaf)	0.041	0.040	0.039	0.042	0.040	0.046	0.045	0.053	0.041
CO (kg/kgdaf)	0.137	0.140	0.109	0.149	0.143	0.159	0.162	0.238	0.162
CO_2 (kg/kgdaf)	0.553	0.617	0.332	0.401	0.403	0.575	0.682	0.428	0.514
C_2H_4 (kg/kgdaf)	0.040	0.039	0.049	0.039	0.039	0.040	0.040	0.044	0.036
C_2H_2 (kg/kgdaf)	0.002	0.001	0.002	0.002	0.002	0.003	0.003	0.002	0.001
C_2H_6 (kg/kgdaf)	0.003	0.003	0.007	0.003	0.004	0.002	0.002	0.006	0.005
C_3H_6 (kg/kgdaf)	0.005	0.005	0.018	0.006	0.005	0.003	0.003	0.009	0.009
C_3H_8 (kg/kgdaf)	0.000	0.000	0.001	0.000	0.000	0.000	0.000	0.001	0.000
Benzene (kg/kgdaf)	0.090	0.107	0.089	0.078	0.101	0.096	0.096	0.063	0.078
Toluene (kg/kgdaf)	0.009	0.011	0.011	0.009	0.012	0.010	0.010	0.008	0.009
Xylenes (kg/kgdaf)	0.000	0.001	0.001	0.000	0.001	0.000	0.000	0.001	0.001
Styrene (kg/kgdaf)	0.006	0.008	0.008	0.007	0.009	0.009	0.009	0.005	0.005
Naphthalene (kg/kgdaf)	0.004	0.006	0.003	0.005	0.006	0.007	0.007	0.004	0.004
Total Arom. (kg/kgdaf)	0.203	0.221	0.173	0.158	0.187	0.174	0.178	0.121	0.137
Char (%C)	19.1	10.7	26.8	23.3	20.4	15.5	12.1	11.2	11.4
Other Aliph (%C)	3.2	7.0	9.5	12.4	11.7	9.0	7.0	10.1	11.6

Other aliphatics (%C) correspond to C4+ aliphatic hydrocarbons.

Total aromatics (%C) include benzene, toluene, xylenes, styrene (BTXS), as well as naphthalene and anthracene, Methylstyrene40, Methylstyrene60, Phenol, 2,3-benzo(b)furan, Aniline, Benzonitrile, Indene, o-Cresol, p-Cresol, Acetophenone, p-Tolunitrile, 1,2-dihydroNaphtalene, Benzoic acid, Naphthalene, 2-MethylNaphthalene, 1-MethylNaphthalene, Biphenyl, Acenaphthylene, Acenaphthene, Dimethyl Terephtalate, Dibenzofuran, 1-naphtol, 2-naphtol, Fluorene, Xantene, Phenantrene, Anthracene, Fluoranthene, Pyrene, Triphenylene as well as a fraction of unknowns. Other aromatic species are not listed explicitly due to their relatively low yields.

Data availability

Data will be made available on request.

References

[1] Textile Exchange, Preferred Fiber & Materials Market Report, 2022. https://textileexchange.org/app/uploads/2022/10/Textile-Exchange_PFMR_2022.pdf (accessed October 25, 2023).
[2] McKinsey Apparel and Fashion & Luxury Group, Scaling textile recycling in Europe-turning waste into value, 2022. https://www.mckinsey.com/industries/retail/our-insights/scaling-textile-recycling-in-europe-turning-waste-into-value#/ (accessed October 26, 2023).
[3] Greenpeace Germany, Poisoned Gifts, 2022.
[4] Dina Lingås (Norion), Saskia Manshoven (VITO), Lars Fogh Mortensen, Freja Paulsen, EU exports of used textiles in Europe's circular economy, 2023. https://www.eea.europa.eu/ds_resolveuid/422c5167f5eb4f62966039b4c90cd26e (accessed October 3, 2024).
[5] Ellen MacArthur Foundation, A NEW TEXTILES ECONOMY: REDESIGNING FASHION'S FUTURE, 2017.
[6] McKinsey & Company and Global Fashion Agenda, FASHION ON CLIMATE HOW THE FASHION INDUSTRY CAN URGENTLY ACT TO REDUCE ITS GREENHOUSE GAS EMISSIONS, 2020. https://www.mckinsey.com/industries/retail/our-insights/fashion-on-climate (accessed October 25, 2023).
[7] Platform for Accelerating the Circular Economy (PACE), The Circularity Gap Report, 2021.
[8] Wang S, Salmon S. Progress toward circularity of polyester and cotton textiles, sustainable. Chemistry 2022;3:376–403. https://doi.org/10.3390/suschem3030024.
[9] Choudhury K, Tsianou M, Alexandridis P. Recycling of blended fabrics for a circular economy of textiles: separation of cotton, polyester, and elastane fibers. Sustainability 2024;16:6206. https://doi.org/10.3390/su16146206.
[10] El Darai T, Ter-Halle A, Blanzat M, Despras G, Sartor V, Bordeau G, et al. Chemical recycling of polyester textile wastes: shifting towards sustainability. Green Chem 2024;26:6857–85. https://doi.org/10.1039/D4GC00911H.
[11] Xie M, Cheng M, Yang Y, Huang Z, Zhou T, Zhao Y, et al. A review on catalytic pyrolysis of textile waste to high-value products: catalytic mechanisms, products application and perspectives. Chem Eng J 2024;498:155120. https://doi.org/10.1016/j.cej.2024.155120.
[12] Yousef S, Eimontas J, Striūgas N, Tatariants M, Abdelnaby MA, Tuckute S, et al. A sustainable bioenergy conversion strategy for textile waste with self-catalysts using mini-pyrolysis plant. Energy Convers Manag 2019;196:688–704. https://doi.org/10.1016/j.enconman.2019.06.050.
[13] Dorado C, Mullen CA, Boateng AA. H-ZSM5 catalyzed co-pyrolysis of biomass and plastics. ACS Sustain Chem Eng 2014;2:301–11. https://doi.org/10.1021/sc400354g.
[14] Tripathi M, Sharma M, Bala S, Thakur VK, Singh A, Dashora K, et al. Recent technologies for transforming textile waste into value-added products: a review. Curr Res Biotechnol 2024;7:100225. https://doi.org/10.1016/j.crbiot.2024.100225.
[15] Mandviwala C, Forero Franco R, Berdugo Vilches T, Gogolev I, González-Arias J, Cañete Vela I, et al. Steam cracking in a semi-industrial dual fluidized bed reactor: tackling the challenges in thermochemical recycling of plastic waste. Chem Eng J 2024;500:156892. https://doi.org/10.1016/j.cej.2024.156892.
[16] Forero-Franco R, Cañete-Vela I, Berdugo-Vilches T, González-Arias J, Maric J, Thunman H, et al. Correlations between product distribution and feedstock composition in thermal cracking processes for mixed plastic waste. Fuel 2023;341:127660. https://doi.org/10.1016/j.fuel.2023.127660.
[17] Cañete Vela I, Maric J, González-Arias J, Seemann M. Feedstock recycling of cable plastic residue via steam cracking on an industrial-scale fluidized bed. Fuel 2024;355:129518. https://doi.org/10.1016/J.FUEL.2023.129518.
[18] Vela IC, Maric J, Seemann M. Valorisation of textile waste via steam gasification in a fluidized bed reactor. Division of Energy Technology, Chalmers University of Technology: Göteborg; 2019.
[19] Li S, Cañete Vela I, Järvinen M, Seemann M. Polyethylene terephthalate (PET) recycling via steam gasification – the effect of operating conditions on gas and tar composition. Waste Manage 2021;130:117–26. https://doi.org/10.1016/j.wasman.2021.05.023.
[20] Song K, Li Y, Wang N, Hou W, Zhang R, Liu J, et al. Co-pyrolysis mechanism of PP and PET under steam atmosphere. J Anal Appl Pyrolysis 2023;173:106033. https://doi.org/10.1016/j.jaap.2023.106033.
[21] Isabel Cañete Vela, Judith Gonzales Arias, Martin Seemann, Chalmers Energy technology, Maria Ström, Wargön innovation, Magnus Rudolfsson, Sveriges lantbruksuniversitet, 4.1.5. Recycling of reject flows from textile sorting and cardboard recycling through thermochemical recycling, 2022.
[22] Isabel Cañete Vela, Martin Seemann, Emma Enebog, Joel Arnoldsson, Hanna de la Motte, Report Thub Project, 2018.
[23] Larsson A, Seemann M, Neves D, Thunman H. Evaluation of performance of industrial-scale dual fluidized bed gasifiers using the chalmers 2–4-MW_{th} gasifier. Energy Fuel 2013;27:6665–80. https://doi.org/10.1021/ef400981j.
[24] Berdugo Vilches T, Thunman H. Experimental investigation of volatiles–bed contact in a 2–4 MWth bubbling bed reactor of a dual fluidized bed gasifier. Energy Fuel 2015;29:6456–64. https://doi.org/10.1021/acs.energyfuels.5b01303.
[25] Mandviwala C, González-Arias J, Berdugo Vilches T, Seemann M, Thunman H. Comparing bed materials for fluidized bed steam cracking of high-density polyethylene: Olivine, bauxite, silica-sand, and feldspar. J Anal Appl Pyrolysis 2023;173:106049. https://doi.org/10.1016/j.jaap.2023.106049.
[26] Israelsson M, Seemann M, Thunman H. Assessment of the solid-phase adsorption method for sampling biomass-derived tar in industrial environments. Energy Fuel 2013;27:7569–78. https://doi.org/10.1021/ef401893j.
[27] Israelsson M, Berdugo Vilches T, Thunman H. Conversion of condensable hydrocarbons in a dual fluidized bed biomass gasifier. Energy Fuel 2015;29:6465–75. https://doi.org/10.1021/acs.energyfuels.5b01291.
[28] Berdugo Vilches T, Lind F, Rydén M, Thunman H. Experience of more than 1000 h of operation with oxygen carriers and solid biomass at large scale. Appl Energy 2017;190:1174–83. https://doi.org/10.1016/j.apenergy.2017.01.032.
[29] Mandviwala C, Forero Franco R, Gogolev I, González-Arias J, Berdugo Vilches T, Cañete Vela IC, Thunman H, Seemann M. Method development and evaluation of product gas mixture from a semi-industrial scale fluidized bed steam cracker with GC-VUV. Fuel Process Technol 2024;253:108030. https://doi.org/10.1016/j.fuproc.2023.108030.
[30] Israelsson M, Larsson A, Thunman H. Online measurement of elemental yields, oxygen transport, condensable compounds, and heating values in gasification systems. Energy Fuel 2014;28:5892–901. https://doi.org/10.1021/ef501433n.
[31] Forero-Franco R, Berdugo-Vilches T, Mandviwala C, Seemann M, Thunman H. Developing a parametric system model to describe the product distribution of steam pyrolysis in a Dual Fluidized bed. Fuel 2023;348:128518. https://doi.org/10.1016/j.fuel.2023.128518.
[32] Altarawneh M, Ali L. Formation of polycyclic aromatic hydrocarbons (PAHs) in thermal systems: a comprehensive mechanistic review. Energy Fuel 2024;38:21735–92. https://doi.org/10.1021/acs.energyfuels.4c03513.
[33] Williams PT, Williams EA. Interaction of plastics in mixed-plastics pyrolysis. Energy Fuel 1999;13:188–96. https://doi.org/10.1021/ef980163x.
[34] Berdugo Vilches T, Marinkovic J, Seemann M, Thunman H. Comparing active bed materials in a dual fluidized bed biomass gasifier: olivine, bauxite, quartz-sand, and ilmenite. Energy Fuel 2016;30:4848–57. https://doi.org/10.1021/acs.energyfuels.6b00327.
[35] Olah GA, Goeppert A, Prakash GKS. Chemical recycling of carbon dioxide to methanol and dimethyl ether: from greenhouse gas to renewable, environmentally carbon neutral fuels and synthetic hydrocarbons. J Org Chem 2009;74:487–98. https://doi.org/10.1021/jo801260f.
[36] Kishi R, Ogihara H, Yoshida-Hirahara M, Shibanuma K, Yamanaka I, Kurokawa H. Green synthesis of methyl formate via electrolysis of pure methanol. ACS Sustain Chem Eng 2020;8:11532–40. https://doi.org/10.1021/acssuschemeng.0c02281.
[37] Olah GA. Beyond oil and gas: the methanol economy. Angew Chem Int Ed 2005;44:2636–9. https://doi.org/10.1002/anie.200462121.
[38] Usman M, Daud WMAW. Recent advances in the methanol synthesis via methane reforming processes. RSC Adv 2015;5:21945–72. https://doi.org/10.1039/C4RA15625K.
[39] Cañete B, Gigola CE, Brignole NB. Synthesis gas processes for methanol production via CH4 reforming with CO2 , H2O, and O2. Ind Eng Chem Res 2014;53:7103–12. https://doi.org/10.1021/ie404425e.
[40] Hankin A, Shah N. Process exploration and assessment for the production of methanol and dimethyl ether from carbon dioxide and water. Sustain Energy Fuels 2017;1:1541–56. https://doi.org/10.1039/C7SE00206H.
[41] Stoll RE, Von Linde F. Hydrogen-what are the costs. Hydrocarbon Process 2000;79:42–6.
[42] Armaroli N, Balzani V. The hydrogen issue. ChemSusChem 2011;4:21–36. https://doi.org/10.1002/cssc.201000182.
[43] Yi Q, Zhao Y, Huang Y, Wei G, Hao Y, Feng J, et al. Life cycle energy-economic-CO2 emissions evaluation of biomass/coal, with and without CO2 capture and storage, in a pulverized fuel combustion power plant in the United Kingdom. Appl Energy 2018;225:258–72. https://doi.org/10.1016/j.apenergy.2018.05.013.
[44] Oh S-Y, Binns M, Cho H, Kim J-K. Energy minimization of MEA-based CO2 capture process. Appl Energy 2016;169:353–62. https://doi.org/10.1016/j.apenergy.2016.02.046.
[45] Thunman H, Berdugo Vilches T, Seemann M, Maric J, Vela IC, Pissot S, et al. Circular use of plastics-transformation of existing petrochemical clusters into thermochemical recycling plants with 100% plastics recovery. Sustain Mater Technol 2019;22:e00124. https://doi.org/10.1016/j.susmat.2019.e00124.
[46] European Comission (EC), Communication from the Commission to the European Parliament, the Council, the European Economic and Social Committee and the Committee of the Regions: EU strategy for sustainable and circular textiles, 2022. https://ec.europa.eu/eurostat.
[47] D. Goldsmith, The Worn, The Torn, The Wearable: textile recycling in Union Square, 2012.
[48] Wagner MM, Heinzel T. Human perceptions of recycled textiles and circular fashion: a systematic literature review. Sustainability 2020;12:10599. https://doi.org/10.3390/su122410599.
[49] Maric J, Berdugo Vilches T, Pissot S, Cañete Vela I, Gyllenhammar M, Seemann M. Emissions of dioxins and furans during steam gasification of Automotive Shredder residue; experiences from the Chalmers 2–4-MW indirect gasifier. Waste Manag 2020;102:114–21. https://doi.org/10.1016/j.wasman.2019.10.037.
[50] Kusenberg M, Eschenbacher A, Djokic MR, Zayoud A, Ragaert K, De Meester S, et al. Opportunities and challenges for the application of post-consumer plastic waste pyrolysis oils as steam cracker feedstocks: to decontaminate or not to

decontaminate? Waste Manag 2022;138:83–115. https://doi.org/10.1016/j.wasman.2021.11.009.
[51] A.K. Roy Choudhury, Environmental Impacts of the Textile Industry and Its Assessment Through Life Cycle Assessment, in: 2014: pp. 1–39. https://doi.org/10.1007/978-981-287-110-7_1.
[52] PLASTICS EUROPE, Plastics the Facts, 2022.